Orientation Invariant Diverstiy Gain Using Transmit Polarization Diversity

Yu Chieh Huang
School of Engineering Systems
Queensland University of Technology
Brisbane, Australia 4000
Email: by.huang@qut.edu.au

Bouchra Senadji
School of Engineering Systems
Queensland University of Technology
Brisbane, Australia 4000
Email: b.senadji@qut.edu.au

***Abstract*—Traditional polarization diversity systems have relied on the distribution of obstacles within the mobile medium to achieve signal decorrelation and power coupling between orthogonal polarizations. If the channel does not facilitate adequate power coupling, signal diversity is suboptimal because signal contribution from the polarization with lesser power is limited. Further, due to the presence of a dominant polarization, the signal power received in the orthogonal polarizations becomes a function of the transmitter orientation. The use of circular polarization at the transmitter is proposed to facilitate power coupling and alleviate the branch power imbalance between the vertical and horizontal polarizations. The analysis shows that if circular polarization is used, the branch power imbalance between the vertical and horizontal polarizations can be significantly lower than linear polarization, and that the cross polarization discrimination becomes independent of the transmitter orientation. The proposed antenna configuration to achieve circular polarization allows for polarization diversity to be implemented in the uplink and downlink.**

I. Introduction

The amplitudes of the signals received in the mobile channel suffer extreme fluctuations as a result of the summation of multipath signals [1]. Signal fades as a result of destructive interference can cause the power of the received signal to drop 30dB below the mean [2], making communications difficult.

Signal based diversity techniques have been well documented in the literature, and are able to effectively alleviate the effects of multipath fading [1]. However, antenna based diversity techniques have been proposed over the signalling based diversity techniques because such techniques do not require the further allocation of spectra, at the expense of additional RF equipment [3]. Traditional antenna space diversity techniques require the physical separation of receiver antenna elements. Due to space availability, the implementation of space diversity may not be possible.

In antenna polarization diversity, antenna elements may be co-located, and signal redundancy is achieved by receiving signals in orthogonal polarizations. Traditional receiver polarization diversity techniques has been realized with the mobile station transmitting a principally vertically polarized signal, and then using a pair of linearly polarized antennas to receive copies of the signal in the vertical polarization (Vpol) and the horizontal polarization (Hpol) [4], [5]. As a result of the multiple reflections and refractions when the signal passes through the mobile medium, some of the signal power in the Vpol is decoupled into the Hpol. Diversity is achieved when the received signals in the Vpol and Hpol exhibit uncorrelated fading.

One of the problems associated with polarization diversity is the branch power imbalance between the Vpol and Hpol. A difference in signal power means that despite having independent fading, diversity benefits are limited because the contribution of the branch with lower power is minimal. In the event that there exists significant difference between mean signal power, no diversity benefits can be gained. The measure of power imbalance in polarization diversity is quantized by the Cross Polarization Discrimination (XPD), and is defined as the ratio between the available power in the vertical polarization and the horizontal polarization. For optimal diversity performance, the XPD $=$ 0dB. The cause of the power imbalance has been hypothesized by Vaughan *et. al* in [5] to be the insufficient number of obstacles within the medium to decouple the power from the principal polarization into the orthogonal polarization, despite being in a dense urban environment. It is reasonable to deduce from this, that if there is insufficient power coupling, then the XPD will change as a function of the transmitter orientation, due to the presence of a dominant polarization.

To compensate for the difference in branch powers, Kozono *et. al* in [4] have proposed a special receiver antenna configuration using two linearly polarized antennas aligned at angles $\pm\alpha$ with respect to the vertical axis. This antenna configuration aims to equalize the mean signal level between the two antennas at the receiver, even if power imbalance exists between the Vpol and Hpol. This equalization however, is at the expense of an increased correlation between the fading signatures in each antenna branch, hence reducing diversity. In the Kozono configuration, the degree of correlation between diversity branches can be controlled by changing the value of α. However, this is at the expense of a reduction of power in both antennas as a result of polarization mismatch. The Kozono antenna configuration compensates for the difference in antenna branch powers, but does not ultimately reduce XPD, which still defines the performance for polarization diversity.

In this paper, we address the problem of power imbalance from the transmitter. The main idea is to use circular polariza-

978-1-4244-4242-3/08/$25.00 ©2008 IEEE

tion at the transmitter to facilitate power coupling, such that there is a component of the electric field in all planes that are orthogonal to the direction of propagation. We show that circular polarization at the transmitter can offer significantly lower power imbalance compared to the traditional linear polarization. The use of circular polarization has the added advantage that the XPD is independent of the transmit antenna orientation.

In Section II, the polarization diversity transmit and receiver systems are described, and channel descriptions are also given. The mathematical derivations for the expression of the XPD as a function of the transmitter orientation is outlined in Section III. Section IV summarizes the results, and presents a comparison of the achievable XPD between linear and circular polarizations. Particular properties of circular polarization will also be presented. Finally, Section V concludes this paper.

II. System Characteristics

A. System Transmitter

At the transmitter, the proposed antenna configuration is made up of two linearly polarized elements V_1 and V_2 which are always orthogonal but are rotatable together. It is assumed that the alignment of the transmit antenna is broadside to the receiver antennas. A circularly polarized signal is produced from this configuration when the transmit signal is fed in quadrature into the antennas. For ease in representation, the signals V_1 and V_2 are presented in complex exponential notation, however only the real component will be transmitted.

$$V_1 = e^{j(\omega t)} \tag{1}$$

$$V_2 = e^{j\left(\omega t - \frac{\pi}{2}\right)}. \tag{2}$$

A Left Hand Circularly (LHC) polarized signal is assumed in this development, however, a Right Hand Circularly (RHC) polarized signal can be easily generated by replacing $V_2 = e^{j\left(\omega t + \frac{\pi}{2}\right)}$. The treatment for a RHC polarized signal is the same as a LHC polarized signal, and yields identical results.

The rotation of the transmit antennas is modelled by using α, which represents the angle between antenna V_1 and the vertical y axis. This configuration is illustrated in Fig. 1. A transformation matrix is used to standardize the arbitrary orientation of the transmitter back into the Vpol and Hpol for analysis, denoted by V_y and V_x respectively.

$$\begin{bmatrix} V_x \\ V_y \end{bmatrix} = \begin{bmatrix} \sin(\alpha) & -\cos(\alpha) \\ \cos(\alpha) & \sin(\alpha) \end{bmatrix} \begin{bmatrix} V_1 \\ V_2 \end{bmatrix} \tag{3}$$

B. Channel

The modelling of the channel is based on the approach taken by Lee *et. al* in [6]. Each element of the **H** matrix corresponds to the complex channel response for each of the transmission links.

$$\mathbf{H} = \begin{bmatrix} \Gamma_{11} e^{j\phi_{11}} & \Gamma_{12} e^{j\phi_{12}} \\ \Gamma_{21} e^{j\phi_{21}} & \Gamma_{22} e^{j\phi_{22}} \end{bmatrix} \tag{4}$$

$\Gamma_{11} e^{j\phi_{11}}$ and $\Gamma_{22} e^{j\phi_{22}}$ represents the Hpol to Hpol and Vpol to Vpol links respectively. While $\Gamma_{21} e^{j\phi_{21}}$ represents the cross coupling from the Vpol to the Hpol, and $\Gamma_{12} e^{j\phi_{12}}$ represents the cross coupling from the Hpol to the Vpol. This configuration is illustrated in Fig. 2. The Γ parameters are the random variables used to model the multipath fading. Given the experimental results published in the literature [6]–[8], weak statistical dependence is assumed between Γ_{11} and Γ_{21} as well as Γ_{22} and Γ_{12}, while statistical independence is assumed across Γ_{11} and Γ_{22}; Γ_{11} and Γ_{12}; Γ_{22} and Γ_{21}, as well as Γ_{12} and Γ_{21}. The ϕ parameters are the result of the random phase introduced by the channel, and are modelled as independent random variables uniformly distributed about $[0, 2\pi)$.

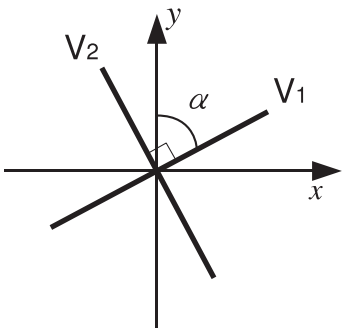

Fig. 1. Transmitter antenna configuration

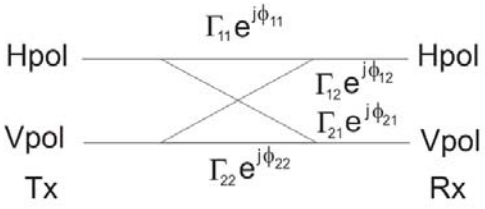

Fig. 2. Channel links between the transmitter and receiver

C. Received signal

At the receiver immediately prior to reception, the resultant signal present in the Vpol and Hpol, given here as R_x and R_y, are written as

$$\begin{bmatrix} R_x \\ R_y \end{bmatrix} = \begin{bmatrix} \Gamma_{11} e^{j\phi_{11}} & \Gamma_{12} e^{j\phi_{12}} \\ \Gamma_{21} e^{j\phi_{21}} & \Gamma_{22} e^{j\phi_{22}} \end{bmatrix} \begin{bmatrix} V_x \\ V_y \end{bmatrix}. \tag{5}$$

Taking only the real part of the signal, the expressions for R_x and R_y are re-written, as it was assumed that only the real part of the signal is actually transmitted. Thus, in the ensuing treatment, the imaginary components will be ignored. R_x and R_y are re-written as

$$\begin{aligned} R_x = \; & \Gamma_{11} \left[\cos(\omega t + \phi_{11}) \sin(\alpha) - \sin(\omega t + \phi_{11}) \cos(\alpha)\right] \\ & + \Gamma_{12} \left[\cos(\omega t + \phi_{12}) \cos(\alpha) + \sin(\omega t + \phi_{12}) \sin(\alpha)\right] \end{aligned} \tag{6}$$

$$R_y = \begin{array}{l} \Gamma_{21}\left[\cos\left(\omega t+\phi_{21}\right)\sin\left(\alpha\right)-\sin\left(\omega t+\phi_{21}\right)\cos\left(\alpha\right)\right] \\ +\Gamma_{22}\left[\cos\left(\omega t+\phi_{22}\right)\cos\left(\alpha\right)+\sin\left(\omega t+\phi_{22}\right)\sin\left(\alpha\right)\right] \end{array} \tag{7}$$

R_x and R_y are then represented in the form to show their inphase and quadrature components.

$$R_x = \begin{array}{l} \left[\Gamma_{11}\sin\left(\alpha-\phi_{11}\right)+\Gamma_{12}\cos\left(\alpha-\phi_{12}\right)\right]\cos\left(\omega t\right) \\ -\left[\Gamma_{11}\cos\left(\alpha-\phi_{11}\right)-\Gamma_{12}\sin\left(\alpha-\phi_{12}\right)\right]\sin\left(\omega t\right) \end{array} \tag{8}$$

$$R_y = \begin{array}{l} \left[\Gamma_{21}\sin\left(\alpha-\phi_{21}\right)+\Gamma_{22}\cos\left(\alpha-\phi_{22}\right)\right]\cos\left(\omega t\right) \\ -\left[\Gamma_{21}\cos\left(\alpha-\phi_{21}\right)-\Gamma_{22}\sin\left(\alpha-\phi_{22}\right)\right]\sin\left(\omega t\right) \end{array} \tag{9}$$

The amplitudes for R_x and R_y are then calculated as

$$\begin{aligned} R_x^2 = & \left[\Gamma_{11}\sin\left(\alpha-\phi_{11}\right)+\Gamma_{12}\cos\left(\alpha-\phi_{12}\right)\right]^2 \\ & +\left[\Gamma_{11}\cos\left(\alpha-\phi_{11}\right)-\Gamma_{12}\sin\left(\alpha-\phi_{12}\right)\right]^2 \\ = & \Gamma_{11}^2+\Gamma_{12}^2+2\Gamma_{11}\Gamma_{12}\sin\left(\phi_{12}-\phi_{11}\right) \end{aligned} \tag{10}$$

$$\begin{aligned} R_y^2 = & \left[\Gamma_{21}\sin\left(\alpha-\phi_{21}\right)+\Gamma_{22}\cos\left(\alpha-\phi_{22}\right)\right]^2 \\ & +\left[\Gamma_{21}\cos\left(\alpha-\phi_{21}\right)-\Gamma_{22}\sin\left(\alpha-\phi_{22}\right)\right]^2 \\ = & \Gamma_{21}^2+\Gamma_{22}^2+2\Gamma_{21}\Gamma_{22}\sin\left(\phi_{22}-\phi_{21}\right) . \end{aligned} \tag{11}$$

III. Derivation of the XPD

The power imbalance between the Vpol and Hpol is measured and quantized by the Cross Polarization Discrimination (XPD). The definition of the XPD is the ratio between the total power in the Vpol and the total power in the Hpol. To calculate the expression for the XPD, we begin by taking the expectation of R_y^2 and R_x^2,

$$E\left[R_x^2\right] = E\left[\Gamma_{11}^2+\Gamma_{12}^2+2\Gamma_{11}\Gamma_{12}\sin\left(\phi_{12}-\phi_{11}\right)\right] \tag{12}$$

$$E\left[R_y^2\right] = E\left[\Gamma_{21}^2+\Gamma_{22}^2+2\Gamma_{21}\Gamma_{22}\sin\left(\phi_{22}-\phi_{21}\right)\right] . \tag{13}$$

Due to the statistical independence between the multipath fading Γ and the random phase ϕ, the expectations can be re-written as

$$E\left[R_x^2\right] = \begin{array}{l} E\left[\Gamma_{11}^2\right]+E\left[\Gamma_{12}^2\right] \\ +2E\left[\Gamma_{11}\right]E\left[\Gamma_{12}\right]E\left[\sin\left(\phi_{12}-\phi_{11}\right)\right] \end{array} \tag{14}$$

$$E\left[R_y^2\right] = \begin{array}{l} E\left[\Gamma_{21}^2\right]+E\left[\Gamma_{22}^2\right] \\ +2E\left[\Gamma_{21}\right]E\left[\Gamma_{22}\right]E\left[\sin\left(\phi_{22}-\phi_{21}\right)\right] . \end{array} \tag{15}$$

The expectation of $\sin\left(\phi_{12}-\phi_{11}\right)$ and $\sin\left(\phi_{22}-\phi_{21}\right)$ is zero because the random phase introduced by each of the channels is modelled as independent random variables, which are uniformly distributed between $[0, 2\pi)$. As a result, the expressions for $E\left[R_y^2\right]$ and $E\left[R_x^2\right]$ simplify down to

$$E\left[R_x^2\right] = E\left[\Gamma_{11}^2\right]+E\left[\Gamma_{12}^2\right] \tag{16}$$

$$E\left[R_y^2\right] = E\left[\Gamma_{21}^2\right]+E\left[\Gamma_{22}^2\right] . \tag{17}$$

To obtain the expression of the XPD, the ratio between $E\left[R_y^2\right]$ and $E\left[R_x^2\right]$ is taken.

$$\text{XPD} = \frac{E\left[R_y^2\right]}{E\left[R_x^2\right]} = \frac{E\left[\Gamma_{22}^2\right]+E\left[\Gamma_{21}^2\right]}{E\left[\Gamma_{11}^2\right]+E\left[\Gamma_{12}^2\right]} \tag{18}$$

The analysis indicates that the use of circular polarization makes the XPD independent of the transmitter orientation. Further, the interpretation of (18) is that in the vertical branch, the total contribution of power is the sum of power contributions from the direct Vpol to Vpol link as well as the cross coupled Hpol to Vpol link. Similarly, the total power in the horizontal branch is the combined contribution from the direct Hpol to Hpol link as well as the cross coupled Vpol to Hpol link.

It is important to note that if a principally vertically polarized signal was assumed at the transmitter, such that $V_2 = 0$ and $\alpha = 0$, the result of the XPD reduces to

$$\text{XPD}_{\text{Vpol}} = \frac{E\left[\Gamma_{22}^2\right]}{E\left[\Gamma_{12}^2\right]} , \tag{19}$$

which holds the same definition of the XPD as the publications in the literature [4] [5], where the treatments were restricted to the use of a principally vertically polarized signal at the transmitter.

An interpretation of (19) is that this represents the magnitude of the power coupling between the Vpol to Vpol and Vpol to Hpol links. A similar expression representing the magnitude of the power coupling between the Hpol to Hpol and Hpol to Vpol links can be obtained by using a principally horizontally polarized signal, and defining $\alpha = \pi/2$ and $V_2 = 0$, such that

$$\text{XPD}_{\text{Hpol}} = \frac{E\left[\Gamma_{21}^2\right]}{E\left[\Gamma_{11}^2\right]} . \tag{20}$$

In general, the magnitude of the power coupling between the vertical and horizontal polarizations is not the same, and depends upon the conditions of the channel. In the following development, for the sake of simplicity, power coupling between the polarizations are assumed to be symmetrical, and is to be quantized by a single parameter χ, such that

$$\begin{aligned} \chi = \text{XPD}_{\text{Vpol}} &= \frac{1}{\text{XPD}_{\text{Hpol}}} \\ &= \frac{E\left[\Gamma_{22}^2\right]}{E\left[\Gamma_{12}^2\right]} = \frac{E\left[\Gamma_{11}^2\right]}{E\left[\Gamma_{21}^2\right]} . \end{aligned} \tag{21}$$

When linear polarization is used, if the channel does not induce power coupling between the polarizations, χ becomes very large as the contributions of $E\left[\Gamma_{12}^2\right]$ and $E\left[\Gamma_{21}^2\right]$ are very small. As a consequence, the obtainable diversity benefits are limited because the power contribution from the orthogonal

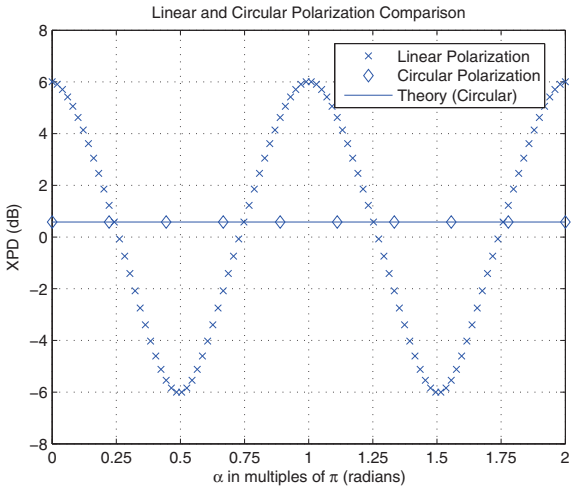

Fig. 3. A comparison of the simulated XPD as a function of transmitter orientation between linear polarization and circular polarization.

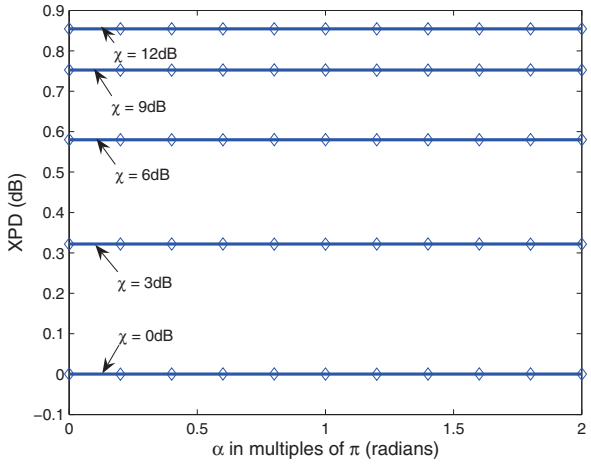

Fig. 4. The comparison between numerically simulated results and the analytical expression for the XPD as a function of transmitter orientation. The different lines represent the cases of cross coupling between polarizations that were considered (χ =0dB, 3dB, 6dB, 9dB and 12dB). XPD_{Asym} = 1dB is assumed.

polarization is minimal. On the other hand, if circular polarization is used, even in the extreme scenario where $E\left[\Gamma_{12}^2\right]$ and $E\left[\Gamma_{21}^2\right]$ approaches zero, the XPD reduces to

$$\text{XPD}_{\text{Asym}} = \frac{E\left[\Gamma_{22}^2\right]}{E\left[\Gamma_{11}^2\right]}. \tag{22}$$

In [9], it was explained that polarizations which are orthogonal to channel obstacles will be attenuated more than the polarizations parallel to the obstacles, as a result, in urban environments, signals in the Hpol are expected to suffer slightly more attenuation than the signals in the Vpol. Equation (22) indicates that for circular polarization, in the extreme case that power coupling between polarizations is absent, the value of the XPD is completely defined by this asymmetric fading between the Vpol and Hpol.

IV. Results

Computer simulations were used to verify the validity of the development. The multipath fading parameters Γ were assumed to be Rayleigh distributed, because this is considered to be the worst case scenario for short term fading [10]. The simulation was set up such that the conditions reflect the channel characteristics which have been measured in the literature [5], [6], [4], [11]. Weak statistical dependence is assumed between Γ_{11} and Γ_{21}, as well as between Γ_{22} and Γ_{12}. The correlation coefficient for both of these combinations were set to 0.15, and these random variables were generated using the method detailed in [12]. Statistical independence is assumed between Γ_{11} and Γ_{22} as well as between Γ_{21} and Γ_{12}. As explained earlier, the signals in the Hpol are expected to suffer slightly more attenuation than the signals in the Vpol [9]. This phenomena is modelled by introducing a small power discrepancy of 1dB between $E\left[\Gamma_{11}^2\right]$ and $E\left[\Gamma_{22}^2\right]$.

Fig. 3 shows the comparison of the achievable XPD between a linearly polarized and a circularly polarized transmitter, for the full range of transmitter orientations. The degree of cross coupling was set to $\chi = 6$dB, and the same channel parameters were used for both simulations. Linear polarization at the transmitter was achieved by setting $V_2 = 0$. Both simulations were realized using 32000 independent trials, however, the procedure was modified slightly to give more resolution in α for linear polarization. The theoretical XPD for circular polarization is also presented, and results in this section indicates that simulations agree closely with the theoretical calculations.

For the same channel conditions, we show that the achievable XPD for a linearly polarized transmitter is dependent upon the antenna orientation, and that a large variation is to be expected. It is important to note that if the linearly polarized transmit antenna was inclined at an of $\alpha = \pi/4$, then the value obtained for the XPD is the same as those obtained for circular polarization. An interesting feature to point out is that if the value of α for the linearly polarized antenna was increased slightly beyond $\pi/4$, the ideal XPD of 0dB may be achieved. The interpretation for this finding is that when the principal polarization is at an angle of $\pi/4$ relative to the y axis, uniform power coupling into the Vpol and Hpol is most easily achieved, moverover, by deliberately increasing the antenna angle past $\pi/4$, more power can be injected into the Hpol to compensate for the asymmetric attenuation between the Vpol and Hpol.

In the mobile uplink, it is unrealistic to assume that the orientation of the transmitter remains unchanged over the duration of the call. This means that even though the ideal XPD of 0dB may be obtained with linear polarization, a small variation in the transmitter orientation can quickly degrade the achievable XPD, hence reduce the performance of polarization diversity.

Fig. 4 shows the comparison between the numerical sim-

ulation and the theoretical expression of the XPD over the full range of angles for the transmit antenna orientation, given different magnitudes of power coupling χ. Cases for χ =0dB, 3dB, 6dB, 9dB and 12dB were tested, and 32000 trials were conducted for each case. As shown, the analytical expression agrees very closely to the simulated results. This verifies that if circular polarization is used at the transmitter, then a fixed XPD can be achieved independent of transmit antenna orientation. Even in the case for $\chi = 12$dB where power coupling across the polarizations is not facilitated, the achievable XPD remains suitably close to 0dB.

V. Conclusion

In this paper, we have considered a polarization diversity system which used circular polarization at the transmitter to facilitate power coupling and compensate for the large power imbalance between the Vpol and the Hpol at the receiver. The main idea is to facilitate power coupling between polarizations by transmitting a component of the electric field in all planes that are orthogonal to the direction of propagation. It is shown that when a circularly polarized signal is transmitted, the resultant XPD remains independent of the transmitter orientation. Further, through simulation, it was shown that circular polarization can offer significantly lower levels of power imbalance compared to linear polarization. The antenna architecture described using two linearly polarized antenna elements which are always orthogonal to generate the circularly polarized signal is advantageous because the same set of antennas may be used as independent linearly polarized elements in a receiver polarization diversity system. Consequently, not only do we get the diversity benefits of a reduced XPD, polarization diversity is now readily realizable in both the uplink and the downlink.

References

[1] W. C. Jakes, *Microwave mobile communications*. Piscataway, N.J : IEEE Press, [1994], c1974., 1974.

[2] V. Fung, T. S. Rappaport, and B. Thoma, "Bit error simulation for Π/4 dqpsk mobile radio communications using two-ray and measurement-based impulse response models," *Selected Areas in Communications, IEEE Journal on*, vol. 11, no. 3, pp. 393–405, 1993.

[3] R. G. Vaughan and J. B. Andersen, "Antenna diversity in mobile communications," *Vehicular Technology, IEEE Transactions on*, vol. 36, no. 4, pp. 149–172, 1987.

[4] S. Kozono, T. Tsuruhara, and M. Sakamoto, "Base station polarization diversity reception for mobile radio," *Vehicular Technology, IEEE Transactions on*, vol. 33, no. 4, pp. 301–306, 1984.

[5] R. G. Vaughan, "Polarization diversity in mobile communications," *Vehicular Technology, IEEE Transactions on*, vol. 39, no. 3, pp. 177–186, 1990.

[6] W. Lee and Y. Yeh, "Polarization diversity system for mobile radio," *Communications, IEEE Transactions on [legacy, pre - 1988]*, vol. 20, no. 5, pp. 912–923, 1972.

[7] T. B. Sorensen, A. O. Nielsen, P. E. Mogensen, M. Tolstrup, and K. Steffensen, "Performance of two-branch polarisation antenna diversity in an operational gsm network," in *Vehicular Technology Conference, 1998. VTC 98. 48th IEEE*, vol. 2, 1998, pp. 741–746.

[8] J. Lempianen, J. Laiho-Steffens, and A. Wacker, "Experimental results of cross polarization discrimination and signal correlation values for a polarization diversity scheme," *Vehicular Technology Conference, 1997 IEEE 47th*, vol. 3, pp. 1498–1502 vol.3, 4-7 May 1997.

[9] J. Jootar, J. F. Diouris, and J. R. Zeidler, "Performance of polarization diversity in correlated nakagami-m fading channels," *Vehicular Technology, IEEE Transactions on*, vol. 55, no. 1, pp. 128–136, 2006.

[10] R. G. Vaughan, "Signals in mobile communications: A review," *Vehicular Technology, IEEE Transactions on*, vol. 35, no. 4, pp. 133–145, 1986.

[11] C. B. Dietrich, K. Dietze, J. R. Nealy, and W. L. Stutzman, "Spatial, polarization, and pattern diversity for wireless handheld terminals," *Antennas and Propagation, IEEE Transactions on*, vol. 49, no. 9, pp. 1271–1281, 2001.

[12] R. B. Ertel and J. H. Reed, "Generation of two equal power correlated rayleigh fading envelopes," *Communications Letters, IEEE*, vol. 2, no. 10, pp. 276–278, 1998.